Induced pluripotent stem cells derived from human intervertebral disc cell for ameliorating neurologic dysfunctions after spinal cord injury

Jinsoo Oh

Department of Medical Science

The Graduate School, Yonsei University

Induced pluripotent stem cells derived from human intervertebral disc cell for ameliorating neurologic dysfunctions after spinal cord injury

Directed by Professor Do Heum Yoon

The Doctoral Dissertation
submitted to the Department of Medical Science,
the Graduate School of Yonsei University
in partial fulfillment of the requirements for the degree
of Doctor of Philosophy

Jinsoo Oh

June 2014

This certifies that the Doctoral Dissertation of Jinsoo Oh is approved.

Thesis Supervisor: Do Heum Yoon

Thesis Committee Member#1: Keung Nyun Kim

Thesis Committee Member#2: Yoon Ha

Thesis Committee Member#3: Tae Il Kim

Thesis Committee Member#4: Sang Hoon Ahn

The Graduate School
Yonsei University

June 2014

ACKNOWLEDGEMENTS

저의 박사 학위 논문을 완성하기까지 많은 도움을 주신 윤도흠, 김긍년, 하윤, 김태일, 안상훈 교수님, 그리고 차의과대학의 황동연 교수님과 이강인 선생님께 다시 한번 깊이 감사 드리며, 차려화, 이혜영, 이혜란, 윤여민 선생님 그리고 휴일도 없이 수많은 시행착오를 거듭하면서도 끝까지 저와 함께 해주었던 유영상 선생님에게 고마움을 전합니다. 또한 아버지와 어머니, 장인 장모님, 동생, 처제, 그리고 사랑하는 아들 지원이와 이 기쁨을 함께 하고 싶습니다.

박사 학위 과정 기간 동안 대학원생으로, 남편으로, 아버지로 그리고 한 가정의 가장으로서 역할을 해오면서 아내에게 경제적으로 큰 힘이 되어 주지 못했다라는 것에 대한 미안함이 늘 마음 한 구석에 자리잡고 있었던 것 같습니다. 오랜 박사 학위 과정 동안 무한한 내조와 사랑으로 저와 가족을 뒷바라지 해준 사랑하는 아내에게 깊은 감사의 마음을 전하며 글을 마칩니다.

<TABLE OF CONTENTS>

<LIST OF FIGURES>

<LIST OF TABLES>

ABSTRACT

Induced pluripotent stem cells derived from human intervertebral disc cell for ameliorating neurologic dysfunctions after spinal cord injury

Jinsoo Oh

Department of Medical Science
The Graduate School, Yonsei University

(Directed by Professor Do Heum Yoon)

Induced pluripotent stem cells (iPSCs) have emerged as a promising cell source for immune-compatible cell therapy. A variety of somatic cells, such as skin fibroblasts and blood cells, have been used to generate iPSCs. However, the most of spinal cord injury (SCI) is caused by spine fracture. During emergency surgery on SCI patients, this disc tissue is often removed as to-be-discarded "waste". In this study, we generated iPSCs from human intervertebral disc cells obtained from patients with spinal cord injury during spine fusion surgery. We investigated the pluripotency of disc cell-derived iPSCs (diPSCs) and neural differentiation capability as well as therapeutic effect to evaluate whether disc cells are suitable as a material of patient-specific iPSC generation for the treatment of spinal cord injury.

Through various analyzes, we confirmed that the diPSCs showed similar characteristics to human embryonic stem cells and were efficiently differentiated into neural progenitor cells (NPCs) with the capability of differentiation into mature neurons *in vitro*. To examine whether the transplantation of NPCs derived from diPSCs had therapeutic effects, NPCs were transplanted into mice 9 days after spinal

cord injury. We detected a significant amelioration of hindlimb dysfunction during follow-up recovery periods. Histological analysis 5 weeks post-transplantation identified undifferentiated human NPCs (nestin^{+}) as well as early (TUJ1^{+}) and mature neurons (MAP2^{+}) derived from NPCs. Furthermore, NPC transplantation demonstrated a preventive effect on spinal cord degeneration resulting from the secondary injury.

In this study, we demonstrated that intervertebral discs removed during surgery, previously considered a “waste” tissue, are able to reuse for patient-specific iPSC generation, and showed the treatability of NPC derived from diPSCs in SCI model.

Key words: intervertebral disc cells, induced pluripotent stem cells, neural progenitor cells, transplantation, spinal cord injury

Induced pluripotent stem cells derived from human intervertebral disc cell for ameliorating neurologic dysfunctions after spinal cord injury

Jinsoo Oh

Department of Medical Science
The Graduate School, Yonsei University

(Directed by Professor Do Heum Yoon)

I. INTRODUCTION

The advent of induced pluripotent stem cells (iPSCs) opened a new avenue for immune-compatible cell replacement therapy as well as *in vitro* disease modeling, drug discovery, and toxicity testing [1-4]. Until now, most iPSCs have been generated using fibroblasts [5], keratinocytes [6], adipose-derived stromal cells [7], and peripheral blood cells [8-10]. However, obtaining somatic cells requires additional painful sampling procedures for patients already suffering from unexpected and sudden trauma such as spinal cord injury. Therefore, it would be convenient and practical to use tissues removed during emergency surgery to generate iPSCs for autologous cell replacement therapy.

Spinal cord injury (SCI) is caused by spine fracture often resulting from a sports injury, traffic accident, or fall. In any case, the fractured spinal vertebra and intervertebral disc are to be removed by spinal stabilization surgery. Therefore, the dissected tissues may be a useful source for iPSC generation. Furthermore, the tissues and cell types obtained in this case are difficult to obtain with a normal biopsy, providing a unique opportunity for evaluating these cell types as a source for iPSC

generation.

Cell therapy using human pluripotent stem cells (hPSCs), such as human embryonic stem cells (hESCs) and iPSCs, is a promising therapeutic approach for patients suffering from spinal cord injury. Several reports confirmed the efficacy of hPSC transplantation using animal models of SCI [11, 12]. Furthermore, Geron Corporation initiated the first hESC-based clinical trials in 2010, although the study was discontinued in 2011 due to financial reasons [11, 12].

In this study, we sought to generate iPSCs using human intervertebral disc cells removed during surgery on SCI patients. We demonstrated that intervertebral discs removed during surgery, previously considered a "waste" tissue, are able to reuse for patient-specific iPSC generation, and showed the treatability of NPC derived from diPSCs in SCI model. This study reported the first generation of hiPSCs from human intervertebral discs and provided a good example of harnessing "waste" surgical tissue to generate iPSCs for future autologous therapy.

II. MATERIALS AND METHODS

1. Isolation of Human Disc Cells

This study was approved by the Institutional Review Board of Yonsei University. Dissected disc tissue was washed with 1X phosphate buffered saline (1X PBS) (Wellgene, Daegu, Korea), then incubated with collagenase A (Roche, Mannheim, Germany) for 4 hours with shaking every hour. The enzyme-treated tissue was filtered through 100-μm mesh, washed three times with 1X PBS, and finally resuspended in DMEM/F12 (Invitrogen, Carlsbad, CA, USA) supplemented with 10% fetal bovine serum (FBS) (Hyclone, Logan, UT, USA) and 1% penicillin/streptomycin (P/S) (Invitrogen) for incubation in a humidified chamber (37^oC, 5% CO_2).

2. Production of Retroviruses

Twenty-four hours before transfection, 293T cells were seeded onto 10-cm culture dishes at a density of $5x10^4$ cells/cm^2 and cultured overnight in an incubator (37^oC, 5%

CO_2). For transfection, 3μg each of four recombinant Moloney-based retroviral vectors (pMXs) expressing human Octamer-binding transcription factor 4 (*Oct4)*, SRY (sex determining region)-box 2 (*Sox2)*, Kruppel-like factor 4 (*Klf4)*, and *c-Myc* genes, 2μg of pGag/Pol, and 1μg of pVSV-G were mixed with Convoy™ Transfection Reagent (ACTGene, Piscataway, NJ, USA) and added to cells of approximately 80-90% confluence, following the manufacturer's suggestions. Medium was changed the next morning and collected 2 days later, followed by ultracentrifugation (64,000 x g, 4°C, 90 min) for harvesting viruses. Viruses in the pellet were resuspended in 0.1ml of 1X PBS and used for transduction.

3. Generation of iPSCs

Approximately $5x10^4$ disc cells were seeded in a 6-well plate with 3 ml of medium consisting of DMEM, 10% FBS, and 1% P/S (all from Invitrogen). After approximately 8-12 hours, the disc cells were treated with the retroviral solution with addition of protamine sulfate (5μg/ml) (Sigma-Aldrich, St. Louis, MO, USA) and subjected to further incubation for 14-16 hours. The next day, the cells were washed three times with 1X PBS (Welgene), and 3 ml of fresh medium was added. Five days after viral transduction, the disc cells were transferred into 6-cm vitronectin-coated dishes at a density of $1\text{-}3x10^4$ cells/dish and were cultured two more days in the disc cell culture medium, followed by further incubation with daily change of the extracelluar matrix-based hPSC medium, as previously established [13]. ESC-like colonies were selected as a clone at approximately 20-25 days and were subjected to expansion.

4. Immunocytochemistry

Samples were washed three times with 1X PBS and then fixed for 10 min with 4% paraformaldehyde (PFA)/1X PBS. After being washed with 1X PBS three times for 10 min each, the samples were then treated with a blocking solution (10% normal donkey serum) for 1 hour at room temperature (RT). The samples were subjected to

consecutive treatments with primary and secondary antibodies for 1 hour each at RT. The samples were treated with DAPI (4′,6-diamidino-2-phenylindole) for 5 min after the secondary antibody treatments.

The primary antibodies used in this show in Table 5. The secondary antibodies used in this study include an Alexa Fluor 594 goat anti-mouse IgG (1:500), FITC donkey anti-mouse IgG (1:500), Cy3 donkey anti-rabbit IgG (1:500), FITC donkey anti-rabbit IgG (1:500), and FITC donkey anti-chicken IgY (1:500) (all from Jackson ImmunoResearch, PA, USA).

5. Alkaline Phosphatase (AP) Staining

Human iPSCs were stained for alkaline phosphatase using the Alkaline Phosphatase Detection Kit (Sigma-Aldrich) according to the manufacturer's instructions.

6. DNA Microarray Analysis

Total RNA was isolated using the NucleoSpin RNA II Kit (Macherey-Nagel, Duren, Germany) according to the manufacturer's suggestions, and 2μg of total RNA was utilized for a genome-wide gene expression profiling experiment using the Illumina array (Illumina, San Diego, CA, USA) at Macrogen (Macrogen, Seoul, Korea).

7. DNA Methylation Analysis

The genomic DNA sample was prepared using a DNeasy Tissue Kit (Qiagen, Hilden, Germany) according to the manufacturer's instructions. 2μg of DNA were treated with an EpiTect Bisulfite Kit (Qiagen) following the manufacturer's instructions. The promoter areas of the *Oct4* and *Nanog* genes were amplified by polymerase chain reaction (PCR), subcloned into a TA cloning vector (RBC Bioscience, New Taipei City, Taiwan), and subjected to sequencing analysis.

8. Pluripotency Test *in vitro*

For the *in vitro* examination of pluripotency, both hESCs and iPSCs were

mechanically detached from the plate and cultured in a Petri dish (SPL Life Sciences, Pocheon, Korea) using the embryoid body (EB) medium (DMEM/F12, 10% Knockout^{TM}SR, 1% non-essential amino acid (NEAA), 0.1mM β-mercaptoethanol, and 1% P/S (all from Invitrogen) for 15 days. EBs were attached to Matrigel-coated slides and were immunostained for representative markers of the three germ layers.

9. Teratoma Formation

For teratoma assay, hPSC colonies were mechanically detached and injected into the testes and muscle of a nonobese diabetic/severe combined immunodeficiency (NOD/SCID) mouse. Roughly $2x10^6$ hPSCs from a 6-cm dish were injected into a NOD/SCID mouse. The teratomas were dissected 8-10 weeks later and were subjected to hematoxylin and eosin staining for histological analysis.

10. G-banding Analysis

A G-banding karyotype analysis of hESCs and iPSCs was performed in the Samkwang Medical Laboratories (Smlab, Seoul, Korea).

11. Induction and Culture of Neural Progenitor Cells (NPCs)

diPSC colonies were mechanically dissected into small fragments with subsequent treatment with 2mg/ml collagenase IV (Invitrogen) for 30-60 minutes. The colony fragments were transferred to a 15-ml tube, collected at the bottom of the tube by gravity, resuspended in 1-2ml of fresh medium, and seeded into uncoated, 6-cm bacterial Petridish (SPL Life Sciences). Approximately 200 colony fragments were seeded on a 6-cm bacterial Petridish. The colony fragments were cultured in suspension for four days in the EB medium and were supplemented with dorsomorphin (5μM) (Sigma-Aldrich) and SB431542 (10μM) (Tocris, Bristol, UK).
Fifty to sixty EBs were transferred to a 3-cm Matrigel-coated dish and were cultured for 6 days in neural progenitor (NP) selection medium (DMEM/F12, 1mM L-Glutamine, 1% NEAA, 0.1mM β-mercaptoethanol, 0.5% N2 supplement, basic

fibroblast growth factor (bFGF, 20ng/ml) (CHA Meditech, Seoul, Korea) with medium change every 2 days.

Neural rosettes were mechanically dissected with pulled glass pipette and cultured in 6-cm Matrigel-coated dishes containing NP expansion medium (DMEM/F12, 1mM L-Glutamine, 1% NEAA, 0.1mM β-mercaptoethanol, 0.5% N2 supplement, 2% B27 supplement, and 20ng/ml bFGF). When the transferred rosettes covered approximately 90% of the dishes, they were treated with Accutase (Invitrogen) for passaging.

12. Neuronal Differentiation

For neuronal differentiation, the iPSC-NPCs were plated at $2x10^4$ cells/cm^2 on poly-L-ornithine (20μg/ml)/laminin (10μg/ml) (all from Sigma-Aldrich)-coated 12 mm round glass coverslip. Cells were maintained in neurobasal medium containing 1% P/S, 1X Glutamax, 2% B27 supplement (all from Invitrogen), brain-derived neurotrophic factor (BDNF, 10ng/ml), and glial cell-derived neurotrophic factor (GDNF, 10ng/ml) (all from peprotech) for 21 days. Half of the medium was replaced every two days.

13. Whole-Cell Patch Clamp

The cover slip with cultured cells was transferred to the recording chamber (Warner instrument, CT, USA) and placed on the microscope (Olympus, Tokyo, Japan) while continuously perfused with CSF containing: 124mM NaCl, 3mM KCl, 1.3mM $MgSO_4$, 1.25mM NaH_2PO_4, 26mM $NaHCO_3$, 2.4mM $CaCl_2$-$2H_2O$, and 10mM glucose. The solution was continuously aerated by O_2 95%/CO_2 5% mixed gas at room temperature (RT).

A glass capillary pipette approached the cell surface. After that, negative pressure was provided to let the pipette go giga seal and whole-cell mode. Internal pipette solution contained 115mM K-gluconate, 10mM KCl, 10mM HEPES, 10mM EGTA, 5mM Mg-ATP, and 0.5mM Na^{2+}-GTP, with pH 7.3 and 280-285 mOsm. Holding potential was -60mV. Na^+ current was recorded in voltage clamp mode, and electrical

stimulation was given with a range from -60mV to +50mV (+10mV per each step). After that, cells went to current clamp mode for testing action potential generation. Cells received 15 steps of current (initial level = 0pA, Δ3-10pA per step) according to their membrane capacity. To verify that currents and spikes were mediated by Na^+ channels, tetrodotoxin (TTX, 0.5μM) (Sigma-Aldrich) was added to the bath for 5-10min, and currents and spikes were retested.

14. Spinal Cord Injury and Cell Transplantation

All protocols were approved by the Animal Care and Use Committee of Yonsei University College of Medicine. All experiments were performed according to international guidelines on the ethical use of animals, and the number of animals used was minimized. Adult male ICR mice (35-40g) (Orient Bio, Gyeonggido, Korea) were used for the SCI model. Before surgery, antibiotics (Cefazoline, 20mg/kg) (Yu-han, Seoul, Korea) were injected into the animals. For anesthesia, Zoletil 50 (30mg/kg) (Virbac, Carros, France) and Rompun (10mg/kg) (Bayer Korea, Seoul, Korea) were injected. After anesthesia, laminectomy was performed at the 11^{th} thoracic level. Compression injury (for 10sec) was carried out using 0.2-mm spacer self-closing forceps at the 11^{th} thoracic level. Cell transplantation was performed 9 days after spinal cord injury. Animals were divided into two groups as follows: group 1 (1X PBS injection) and group 2 (diPSC-derived NPCs, $5x10^5$ cells injection). Two microliters of cell suspension containing $5x10^5$ cells were injected into the injury epicenter using a micro injector attached to a pulled glass capillary needle (inner diameter: 150-200μm) at a rate of 1μl/min. For immune suppression, Cyclosporine A (10mg/kg) (Chong Kun Dang, Seoul, Korea) was administered to all animals until sacrifice.

15. Behavior Tests

To confirm whether cell transplantation improved hindlimb functional recovery, the open field locomotor test was performed every week for six weeks using Basso

Mouse Scale (BMS) scoring, and footprint analysis was performed only at the final week. Briefly, both hindlimbs were soaked in paint, and the animals walked on drawing paper. Stride length, stance length, and sway length were measured.

16. Tissue Preparation and Immunofluorescence Staining

Five weeks after cell transplantation, animals were sacrificed by heart perfusion with saline and 4% PFA (Merck, Darmstadt, Germany). Spinal cord tissue was obtained and incubated in 4% PFA for 24 hours at 4^{o}C. After fixation, samples were incubated in 30% sucrose solution at 4^{o}C. Tissues were embedded into optimal cutting temperature (OCT) compound, incubated at -70^{o}C, and cut into slices of 20μm thickness. Immunofluorescence staining was performed as follows. Samples were washed with ice-cold 1X PBS, followed by blocking with 10% normal donkey serum (Jackson ImmunoResearch, PA, USA) in 1X PBS containing 0.3% Triton X-100 (Sigma-Aldrich) for 1 hour at RT. Primary antibodies (Table 5) were treated either for 1 hour at RT or overnight at 4^{o}C. After three washings with ice-cold 1X PBS, fluorescent dye-conjugated secondary antibodies (Jackson ImmunoResearch) were treated for 1 hour at RT. The samples were mounted with mounting solution (Vector Laboratories, Peterborough, UK) and analyzed using an Olympus BX51 fluorescence microscope (Olympus) and LSM 700 confocal microscope (ZEISS, Oberkochen, Germany). The percentage of nestin-, beta-III tubulin (TUJ1)-, microtubule-associated protein 2 (MAP2)-, glial fibrillary acidic protein (GFAP)-, and neuron/glia-type 2 (NG2)-positive cells among human nuclei (HNU)-positive cells within 0.3mm^2 was examined (three independent regions).

17. Statistical Analysis

Student's t-tests were performed to assess differences between the two groups. One-way anova test were performed to assess difference among three groups. The data were presented as the mean ± S.E.M. *p*-values less than 0.05 were considered

statistically significant. All data were analyzed using Medcalc software (MedCalc Software, Ostend, Belgium).

III. RESULTS

1. Isolation of Disc Cells for iPSC Generation from a Patient with SCI

In this study, we examined whether iPSCs could be generated from typically-discarded disc cells isolated from surgically removed human intervertebral discs and whether NPCs differentiated from the disc cell-derived iPSCs (diPSCs) reversed the locomotor dysfunction of an animal SCI model (Fig.1A). A large number of the disc-originated cells in our culture displayed the morphology of nucleus pulposus (NP) cells, which are less elongated and more branched than annulus fibrosus (AF) cells (Fig.1B) [14]. Consistent with this morphological observation, NP marker genes such as *aggrecan* (*ACAN*), *SRY (sex determining region Y)-box 9* (*Sox9*), and *Type II collagen* (*Col2A1*) were abundantly expressed in the disc cell population (Fig.1C) [15].

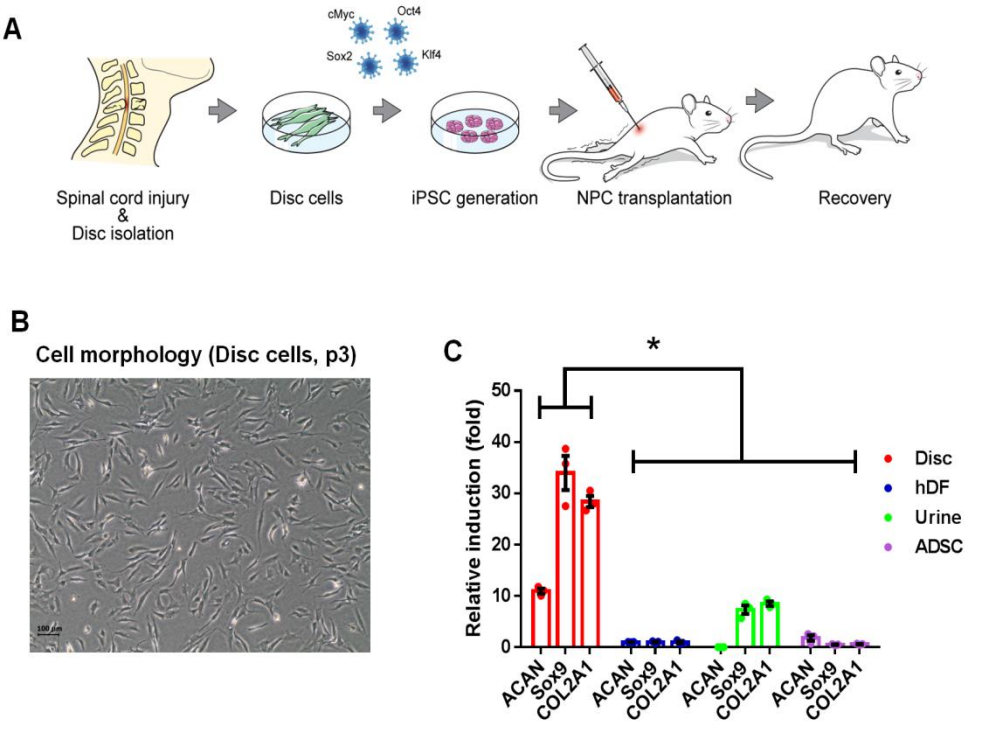

Figure 1. Experimental Design and Characteristics of Human Intervertebral Disc-derived Cells

(A) Schematic illustration of the experimental paradigm adopted in this study. (B) Morphology of the cells (passage 3) derived from human intervertebral discs. (C) Quantitative real-time RT-PCR demonstrated high expression of chondrogenic markers *aggrecan* (*ACAN*), *SRY (sex determining region Y)-box9* (*Sox9*), and *Type II collagen* (*Col2A1*) in the disc cells compared with adult dermal fibroblasts, urine cells, and adipose-derived stromal cells (ADSC). All cell types were analyzed at passage 3. *$p<0.01$ (N=3).

2. Generation and Characterization of diPSCs from the Cultured Disc Cells

hPSC-like colonies appeared approximately 18-20 days after the disc cells were transduced with a mixture of retroviral vectors expressing each of *Oct4*, *Sox2*, *Klf4*, and *c-Myc* genes (Fig.2A). The efficiency of iPSC formation from disc cells was approximately 0.1%. A DNA fingerprinting analysis confirmed that the diPSCs were derived from the original disc cells that were used for the iPSC generation (Table 1). Both immunocytochemistry (Fig.2B) and real-time RT-PCR (Fig.3A) demonstrated that the iPSC lines robustly expressed undifferentiated cell markers Oct4, Sox2, Stage specific embryonic antigen 4 (SSEA4), Tra1-60, Tra1-80, *Nanog*, DNA (cytosine-5-)-methyltransferase 3 beta (*DNMT3B*), Zic family member 3 (*Zic3*), and Zinc finger protein-42 (*Rex1*). On the other hand, low-level expression of representative markers for neuroectoderm (Sex determining region Y-box 1 (*Sox1*) and Paired box 6 (*Pax6*)), mesoderm (GATA binding protein 2 (*Gata2*) and *Brachyury*), and endoderm (Alpha-Fetoprotein (*AFP*) and Sex determining region Y-box 17 (*Sox17*)) was detected (Fig.3B).

G-banding analysis indicated that there were no gross chromosomal aberrations in the diPSCs (Fig.4). Consistent with the high level of *Oct4* and *Nanog* gene expression, the regulatory regions of the two genes were hypomethylated in both diPSCs and hESCs, but not in their original disc cells (Fig.5).

Next, we closely examined global gene expression patterns of diPSCs, H9-hESCs, and disc cells. Scatter plot, correlation matrix, hierarchical clustering, and heatmap analyses all demonstrated that diPSCs had similar gene expression patterns to hESCs, but not to their original disc cells (Fig.6 and 7). As previously reported in many other laboratories, PCR analysis showed that the exogenously delivered *Oct4*, *Sox2*, *Klf4*, and *c-Myc* transgenes were turned off in diPSCs, while their endogenous counterparts were actively expressed (Fig.8). All together, these results indicated that the diPSC colonies formed in our study displayed characteristics similar to hESCs.

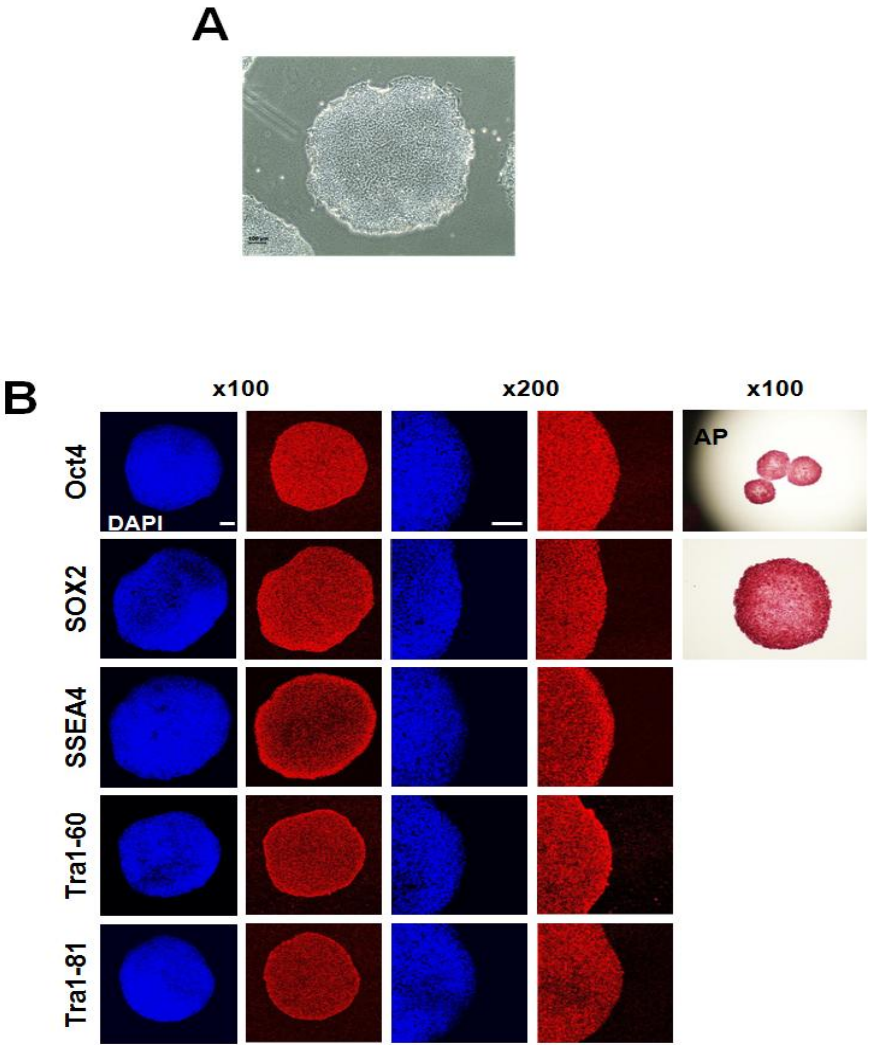

Figure 2. Pluripotent Marker Staining

(A) A phase contrast image of diPSC colonies, which were generated and cultured for 15 passages. (B) diPSC colonies at passage 15 were immunostained with representative pluripotency markers (Tra1-81, Tra1-60, SSEA4, Sox2, and Oct4) and were also stained for alkaline phosphatase.

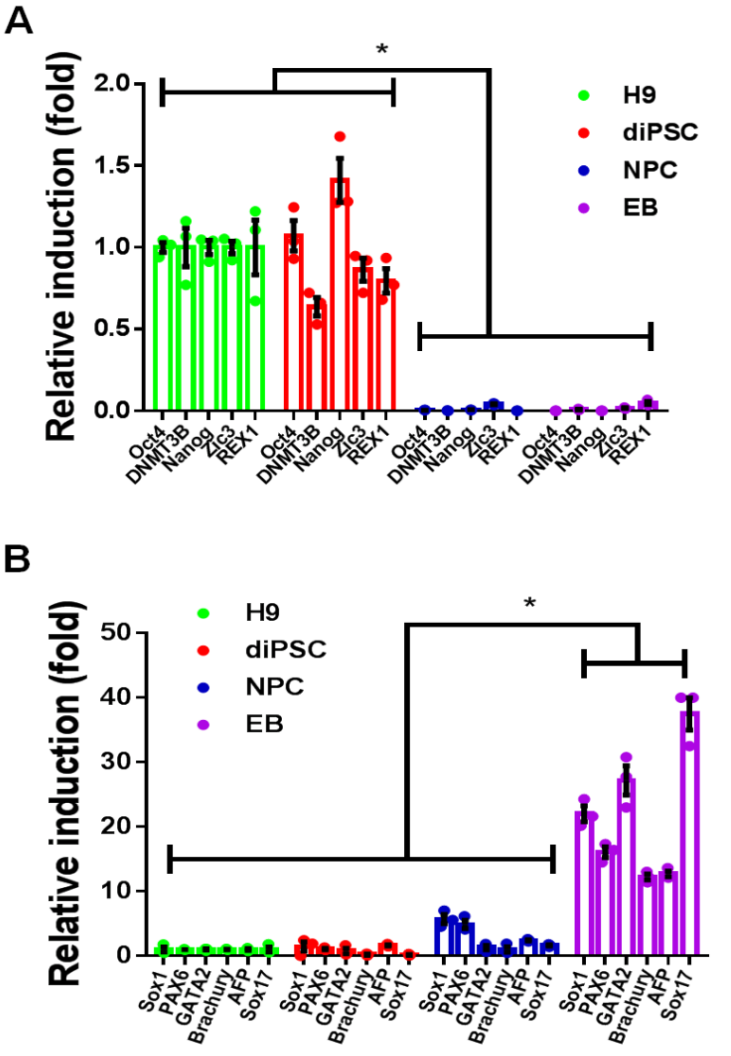

Figure 3. Gene Expression Level, qRT-PCR

(A) Quantitative RT-PCR was performed to detect the levels of multiple undifferentiated cell markers, such as *Oct4*, *DNMT3B*, *Nanog*, *Zic3*, and *Rex1*. *$p<0.01$ (N=3). (B) The expression levels of the representative marker genes for the ectoderm (*Sox1 and Pax6*), mesoderm (*GATA2 and Brachyury*), and endoderm (*AFP and Sox17*) lineages were measured by quantitative RT-PCR. *$p<0.05$. Data are presented as the mean ±S.E.M.

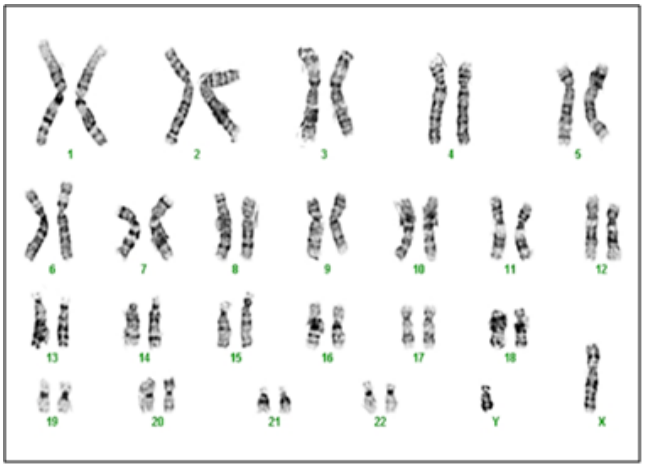

Figure 4. G-banding Analysis

G-banding analysis of diPSC1 at passage 13.

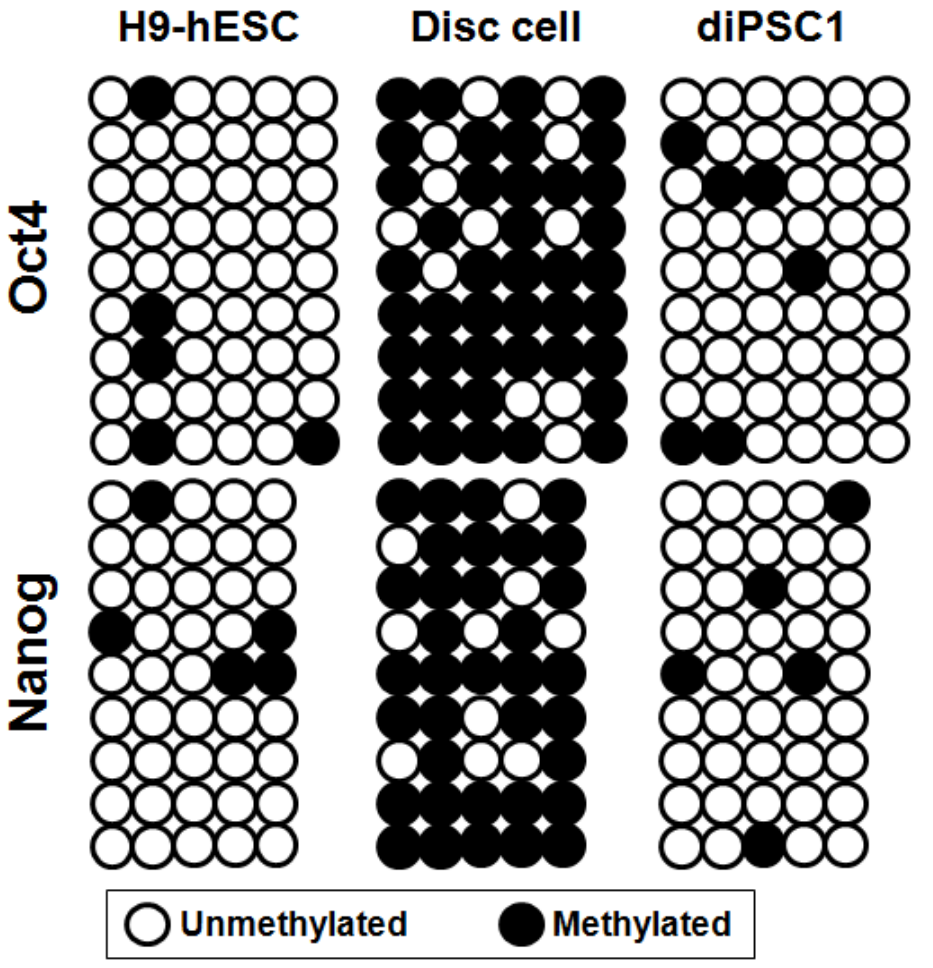

Figure 5. DNA Methylation Analysis

Bisulfite sequencing analysis to examine the methylation pattern of the *Oct4* and *Nanog* promoters in H9-hESCs, disc cells, and diPSC.

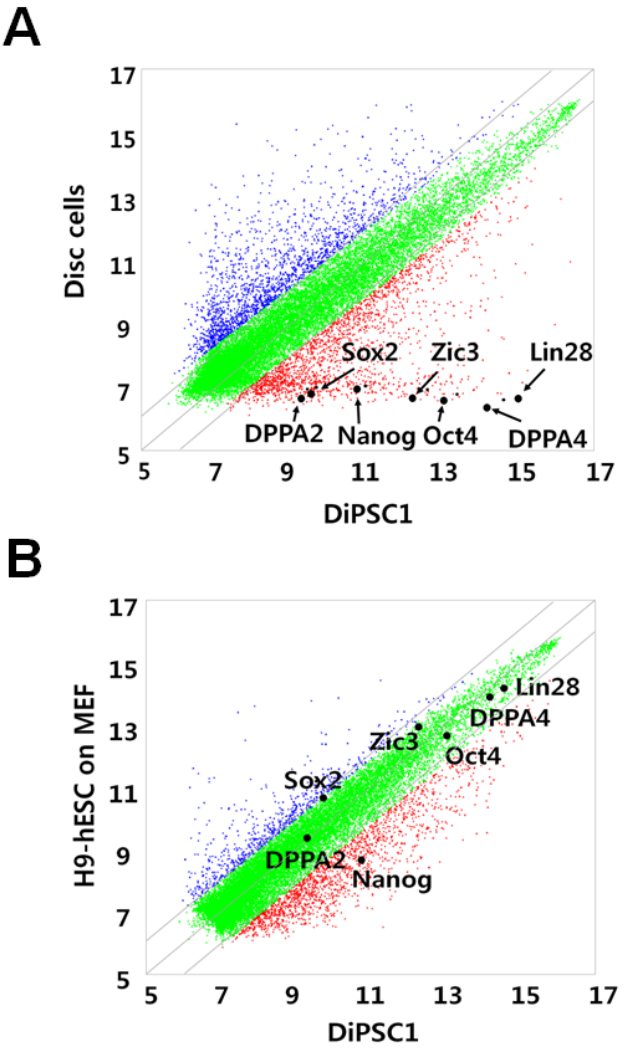

Figure 6. Gene Expression Level, Scatter Plots

The scatter plots compare gene expression levels between disc cells and diPSC1 (A) and between H9-hESCs and diPSC1 (B).

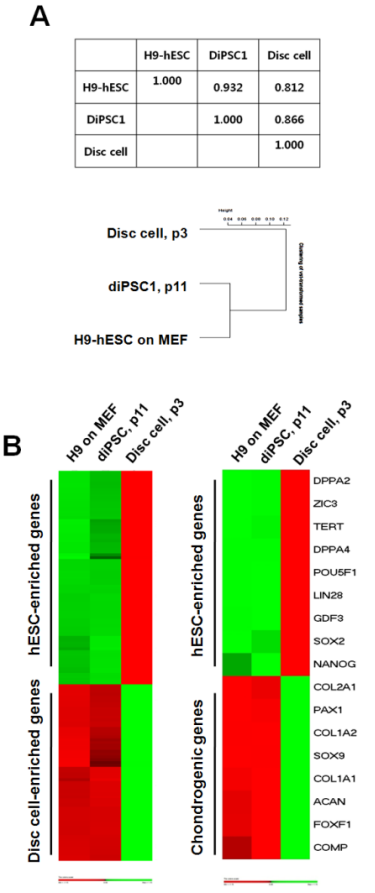

Figure 7. Hierarchical Clustering and DNA Microarray Analysis

(A) Pair-wise Pearson's correlation coefficients among gene expression profile data for H9-hESCs, diPSC1, and disc cells were shown (*top).* Hierarchical clustering of the global expression profiles of H9-hESCs, diPSC1, and disc cells was shown (*bottom*). (B) A heatmap of the expression of the disc cell- and hESC-enriched genes from H9-hESCs, diPSCs (p11), and disc cells (p3) (*left*). The list of disc cell- and hESC-enriched genes is shown in Table 2. In addition, a heatmap of the expression of chondrogenic- and hESC-enriched genes were shown on the right. The list of chondrogenic- and hESC-enriched genes is shown in Table 3. The genes shown in green represent upregulation of expression, whereas the genes in red represent downregulation.

.

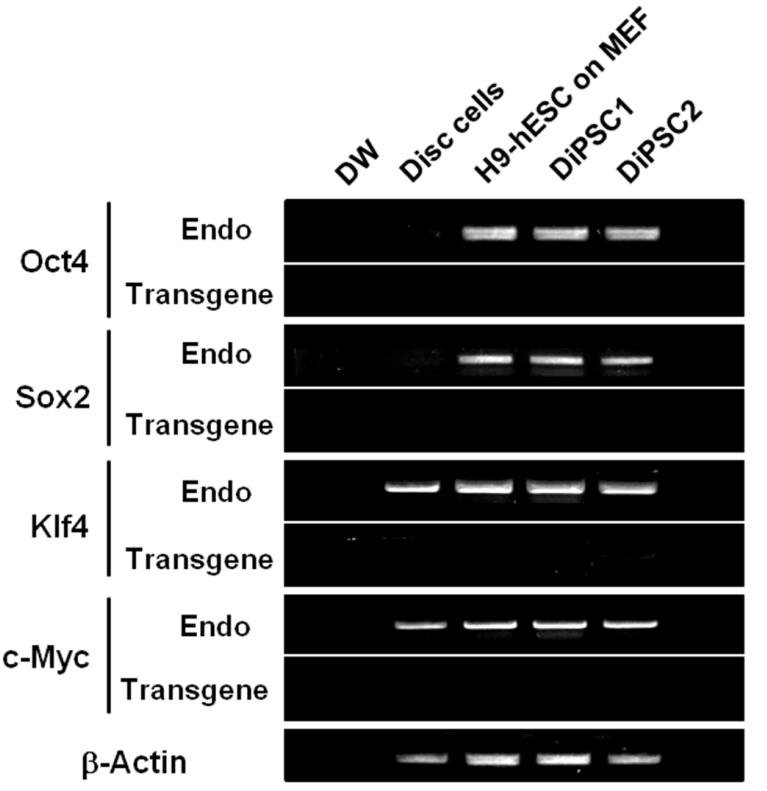

Figure 8. Expression of Transgenes and Endogenous Counterpart

RT-PCR analysis to examine the expression of *Oct4*, *Sox2*, *Klf4*, and *c-Myc* transgenes (Transgene) and their endogenous counterparts (Endo). PCR primer pairs specific for transgenes and endogenous genes were used (the primer sequences were described in Table 4). β-Actin is used as a loading control.

Table 1. DNA Fingerprint Analysis

Locus / sample	Disc cell	diPSC1
D8S1179	12,14	12,14
D21S11	28,31	28,31
D7S820	8,11	8,11
CSF1PO	9,11	9,11
D3S1358	15,17	15,17
TH01	9,9	9,9
D13S317	9,11	9,11
D16S539	12,12	12,12
D2S1338	18,24	18,24
D19S433	15,15.2	15,15.2
vWA	18,18	18,18
TPOX	8,8	8,8
D18S51	12,15	12,15
D5S818	10,10	10,10
FGA	22,22	22,22

Table 2. Lists of hESC- and Disc Cell-enriched Genes shown in Fig.7B (*left*)

hESC-enriched genes	GeneBank	Disc cell-enriched genes	GeneBank
ACTA1	NM_001100.3	*AEBP1*	NM_001129.3
AIF1L	NM_031426.2	*AKR1C2*	NM_001354.4
APOE	NM_000041.2	*ALDH3A1*	NM_000691.3
BEX1	NM_018476.3	*ALPK2*	NM_052947.3
BEX2	NM_032621.2	*ANPEP*	NM_001150.1
C9orf135	NM_001010940.1	*APCDD1L*	NM_153360.1
CACHD1	NM_020925.2	*APPL2*	NM_018171.3
CAMKV	NM_024046.3	*ARID5B*	NM_032199.1
CCND2	NM_001759.2	*ASAP2*	NM_003887.2
CD24	NM_013230.2	*AXL*	NM_021913.2
CDH1	NM_004360.2	*BAPX1*	NM_001189.2
CDH3	NM_001793.3	*C10orf116*	NM_006829.2
CNTNAP2	NM_014141.4	*C14orf78*	XM_001132404.1
CRMP1	NM_001014809.1	*CAMK2N1*	NM_018584.5
CXADR	NM_001338.3	*CAV1*	NM_001753.3
CYP2S1	NM_030622.6	*CAV2*	NM_001233.3
DPPA4	NM_018189.3	*CD44*	NM_001001392.1
EDNRB	NM_000115.1	*CEBPD*	NM_005195.3
EPCAM	NM_002354.2	*COL16A1*	NM_001856.3
FLJ40504	NM_173624.1	*COL6A2*	NM_001849.3
GPC4	NM_001448.2	*COL8A1*	NM_020351.2
GPM6B	NM_001001995.1	*CPA4*	NM_016352.2
HAND1	NM_004821.1	*CYBRD1*	NM_024843.2
HERC5	NM_016323.2	*DAB2*	NM_001343.2
IGF2BP3	NM_006547.2	*DCN*	NM_133505.2
IGFBP2	NM_000597.2	*EFEMP2*	NM_016938.2
KIF1A	NM_004321.4	*FAM129B*	NM_001035534.1
L1TD1	NM_019079.2	*FAM20C*	NM_020223.2
LDB2	NM_001290.2	*FAM38A*	NM_014745.1
LECT1	NM_007015.2	*FBLN5*	NM_006329.2
LIN28	NM_024674.4	*FER1L3*	NM_013451.2
LIN28B	NM_001004317.2	*FGFRL1*	NM_021923.3
LOC642559	XR_016333.1	*FOXC1*	NM_001453.1
LOC643272	XM_926633.1	*FRMD6*	NM_152330.2
LOC645682	XR_017655.1	*GAS6*	NM_000820.1
LRRN1	NM_020873.5	*GAS6*	NM_000820.1
MT1H	NM_005951.2	*GREM1*	NM_013372.5
MYCN	NM_005378.4	*HERC4*	NM_022079.2
NLGN4X	NM_020742.2	*HTRA1*	NM_002775.3
NNAT	NM_181689.1	*IGFBP3*	NM_001013398.1

NTS	NM_006183.3	*IGFBP6*	NM_002178.2
PODXL	NM_001018111.2	*IGFBP7*	NM_001553.1
POU5F1	NM_002701.4	*ITGA3*	NM_002204.1
POU5F1P1	NR_002304.1	*KCNMA1*	NM_002247.2
POU5F1P1	NR_002304.1	*KDELR3*	NM_016657.1
PPP2R2B	NM_181676.1	*KDELR3*	NM_006855.2
PROM1	NM_006017.1	*LMNA*	NM_005572.3
RASL11B	NM_023940.2	*LOC399959*	NR_024430.1
RPRM	NM_019845.2	*LOC645638*	XR_040455.1
SALL4	NM_020436.2	*LOXL3*	NM_032603.2
SBK1	NM_001024401.2	*LPAR1*	NM_057159.2
SEMA6A	NM_020796.3	*LTBR*	NM_002342.1
SFRP2	NM_003013.2	*LXN*	NM_020169.2
SLC7A3	NM_032803.4	*MALL*	NM_005434.3
SOX2	NM_003106.2	*MVP*	NM_005115.3
TACSTD1	NM_002354.1	*MXRA5*	NM_015419.2
TNFRSF21	NM_014452.3	*MYOF*	NM_013451.3
UCA1	NR_015379.2	*NDRG1*	NM_006096.2
ZFP42	NM_174900.3	*OBFC1*	NM_024928.3
ZIC2	NM_007129.2	*PAPSS2*	NM_004670.3
ZIC3	NM_003413.2	*PCOLCE*	NM_002593.2
ZSCAN10	NM_032805.1	*PDGFRB*	NM_002609.3
		PPP1R3C	NM_005398.4
		PTGER2	NM_000956.2
		RPS6KA2	NM_001006932.1
		S100A16	NM_080388.1
		S100A4	NM_019554.2
		SCARA3	NM_016240.2
		SIRPA	NM_001040023.1
		SLFN11	NM_152270.2
		STEAP3	NM_018234.2
		TM4SF1	NM_014220.2
		TMEM166	NM_032181.1
		TSPO	NM_007311.3
		ZAK	NM_133646.2

Table 3. Lists of hESC- and Chondrogenic-enriched Genes shown in Fig.7B (*right*)

hESC-enriched genes	GeneBank	Chondrogenic-enriched genes	GeneBank
DPPA2	NM_138815.2	*COL2A1*	NM_001844.3
ZIC3	NM_003413.2	*PAX1*	NM_006192.1
TERT	NM_198253.2	*COL1A2*	NM_000089.3
DPPA4	NM_018189.3	*SOX9*	NM_000346.2
POU5F1	NM_002701.4	*COL1A1*	NM_000088.3
LIN28	NM_024674.4	*SOX9*	NM_000346.2
GDF3	NM_020634.1	*FOXF1*	NM_001451.2
SOX2	NM_003106.2		
NANOG	NM_024865.2		

3. Pluripotency of diPSCs

In spontaneous differentiation conditions, diPSCs were shown to differentiate into derivatives of all three germ layers, as detected by immunostaining of the following representative germ layer markers: nestin and beta-III tubulin for ectoderm, smooth muscle actin (SMA) and platelet endothelial cell adhesion molecule-1 (PECAM-1) for mesoderm, and alpha-fetoprotein (AFP) and forkhead box A2 (FoxA2) for endoderm (Fig.9A). Furthermore, when injected into NOD/SCID mice, diPSCs formed complex teratomas consisting of tissues derived from all three germ layers (Fig.9B). Taken together, both *in vitro* and *in vivo* results demonstrated that the diPSCs retained the capability of pluripotency.

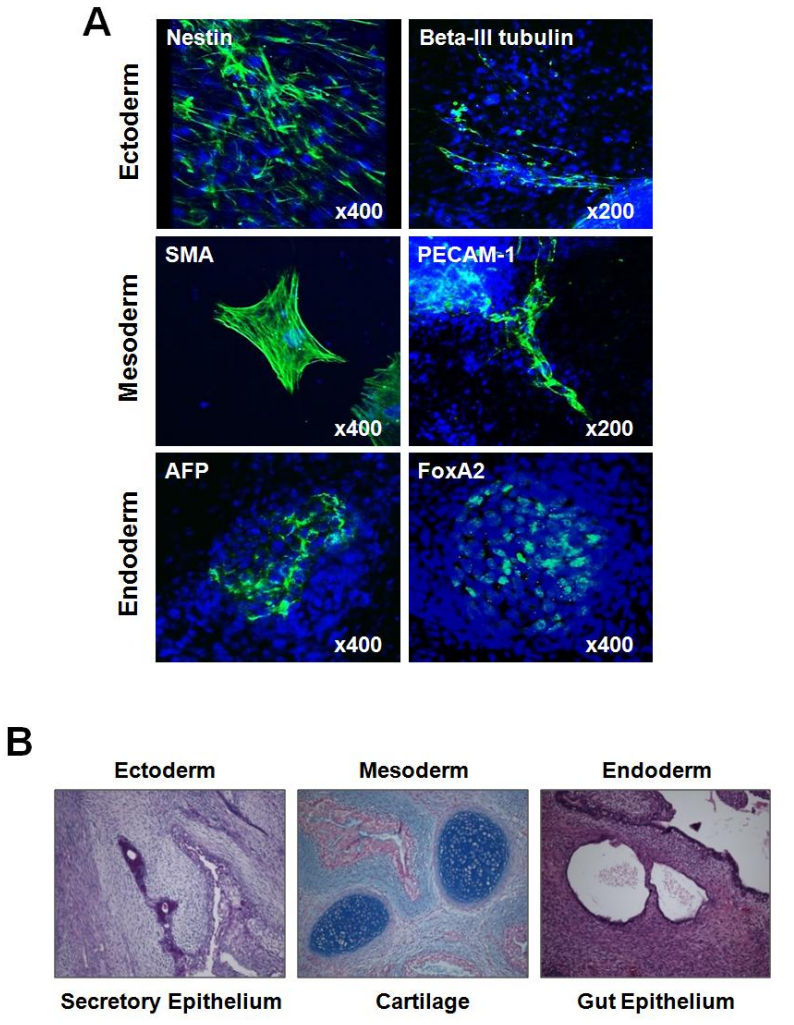

Figure 9. Differentiation of diPSCs into Derivatives of the Three Germ Layers

(A) diPSCs (p15) were spontaneously differentiated *in vitro*, and the expression of representative markers of ectoderm (nestin and beta-III tubulin), mesoderm (SMA and PECAM-1), and endoderm (AFP and FoxA2) were examined. (B) The derivatives of the three germ layers were detected in teratomas approximately 8-10 weeks after administration of diPSCs ($2x10^6$ cells) into NOD/SCID mice.

4. Differentiation of diPSCs into Neural Progenitor Cells (NPCs)

diPSCs were differentiated into NPCs via the previously described EB-based method with slight modifications (Fig.10A) [16]. Neural rosettes were mechanically selected and seeded as a single cell in the neural expansion medium to culture the NPCs. The NPCs were passaged 8 times *in vitro* and robustly expressed NPC makers, such as nestin, Sox2, Pax6, and Sox1 (Fig.10B). Semi-quantitative RT-PCR also showed the expression of both NPC and neural rosette markers in hPSC-derived NPCs (H9-NPCs, diPSC1-NPCs, and diPSC2-NPCs), but not in H9-hESCs and diPSCs (Fig.11).

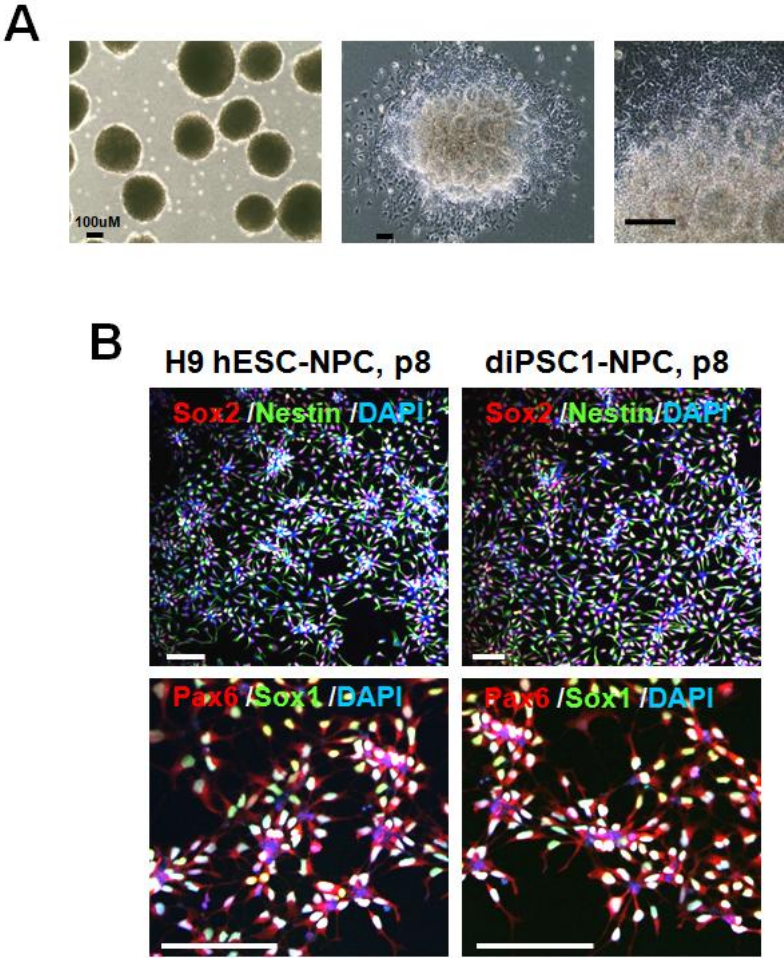

Figure 10. Generation and Characterization of diPSC-NPCs

(A) diPSCs were coaxed into NPCs (diPSC-NPCs) via EB formation in the presence of dorsomorphin (DM) and SB431542 (SB). EBs (*left panel*) and neural rosettes (*middle and right panels*) were shown. (B) The NPCs selected and expanded from neural rosettes were immunostained with neural progenitor markers Sox2, nestin, Sox1, and Pax6. *Bottom* panels are higher magnification images of *top* panels.

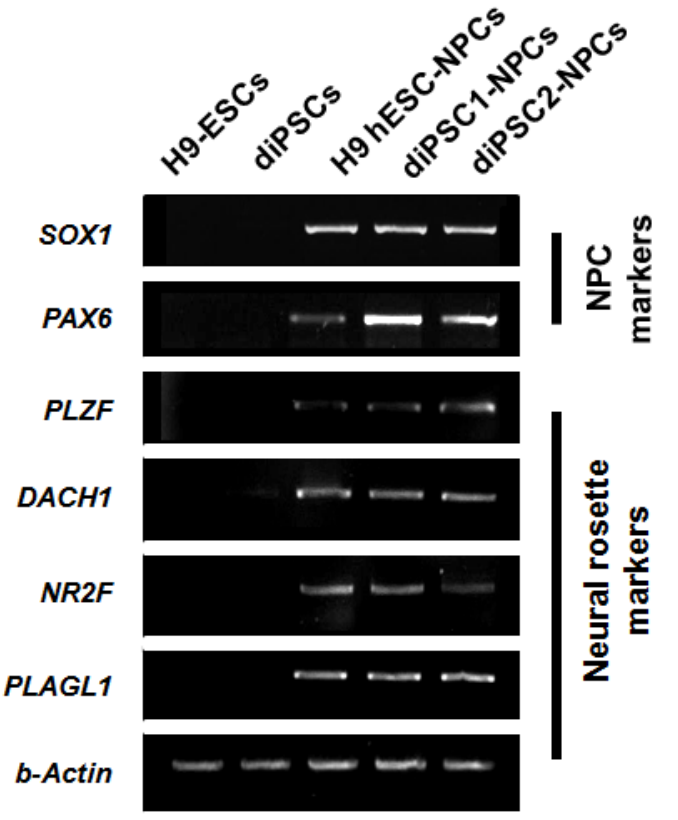

Figure 11. Expression of Marker Specific for NPC and Neural Rosette

RT-PCR analysis showed the expression of markers for both NPCs (*Sox1* and *Pax6*) and neural rosettes (*PLZF*, *DACH1*, *NR2F*, and *PLAGL1*) in NPCs derived from hESCs, diPSC1, and diPSC2.

5. Neuronal Differentiation *in vitro*

Next, we investigated whether the diPSC-NPCs could be further coaxed into neurons *in vitro*. The neurons generated by differentiation of diPSC-NPCs displayed typical neuronal morphology with small soma and long processes (Fig.12A). Twenty-one days after differentiation, most of the neurons were expressing beta-III tubulin ($TUJ1^+$) (Fig.12B and C), microtubule-associated protein 2 (MAP2) (Fig.12D and E), neural cell adhesion molecule (NCAM) (Fig.12F and G), neurofilament heavy (NF-H) (Fig.12H), and neuronal nuclei (NeuN) (Fig.12I). Among them, tyrosine hydroxylase $(TH)^+$ dopaminergic neurons (Fig.12J) and vesicular glutamate transporter 2 $(vGlut2)^+$ glutamatergic neurons (Fig.12K and L) were also detected. The electrophysiological properties of the diPSC-derived neurons were examined by whole-cell patch clamp recordings. In voltage clamp mode, Na^+ currents were found in differentiated neurons (Fig.13A). Cells were held at -60mV, and several current peaks were recorded when sequential stimulations (from -60mV to +50mV) were applied. The maximum peak amplitude was -556.6pA. For confirmation of excitability, another piece of evidence indicating normal neuronal function, we used evoked action potentials in the current clamp mode. Action potential spikes resulted (Fig.13B), but they appeared only in the cells that produced Na^+ currents. This result implied that the action potentials were caused by the same Na^+ channels that elicited positive current in Fig.13A.

To confirm that the channels that produced currents and spikes were Na^+ channels, Na^+ channel antagonist tetrodotoxin (TTX) was added in the bath for 5-10min. TTX blocked Na^+ channels completely, and Na^+ currents and action potential spikes totally disappeared (Fig.13A and B, *right panel*), supporting the assertion that the currents and spikes were mediated by Na^+ channels. diPSC-derived neurons expressed a certain level of Na^+ channels and generated action potentials, indicating that the diPSC-derived NPCs had differentiated into mature neurons.

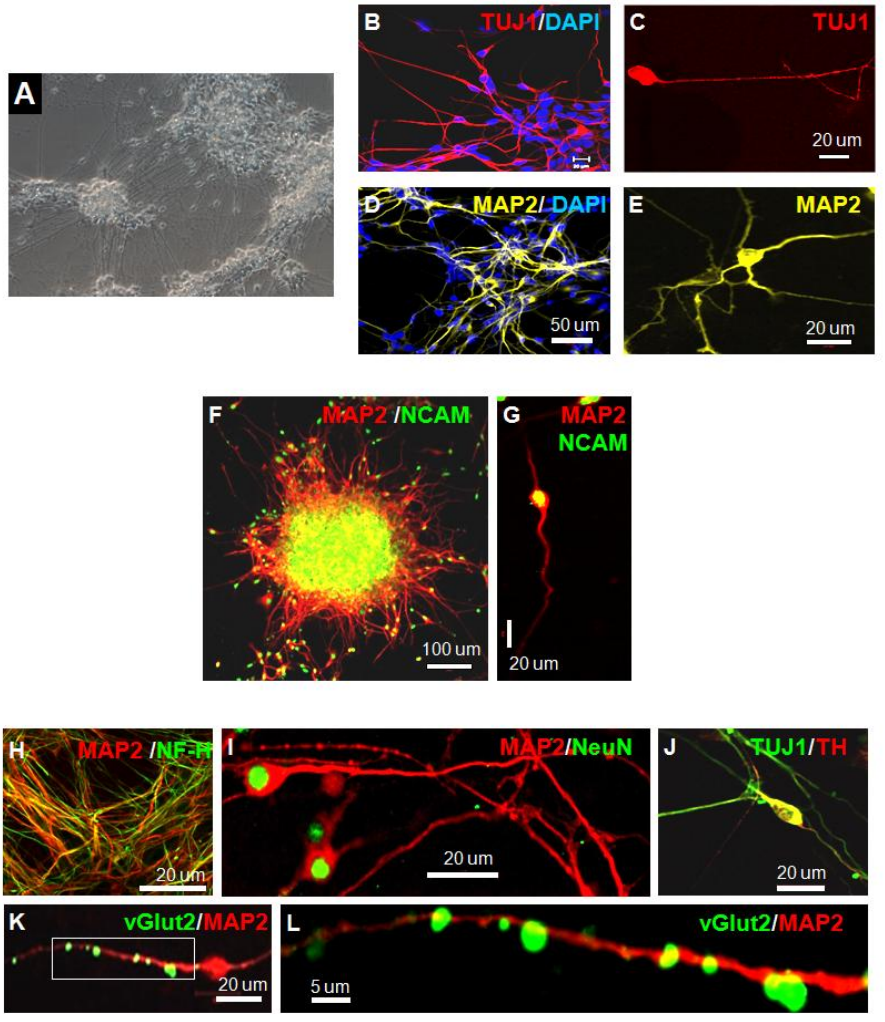

Figure 12. Neuronal Differentiation

(A) A DIC image of neurons differentiated from diPSC-NPCs. (B and C) $TUJ1^+$ neurons at low and high magnifications, respectively. (D and E) $MAP2^+$ neurons at low and high magnifications, respectively. (F and G) $NCAM^+$ neurons at low and high magnifications, respectively. (H) Dense $NF^+/MAP2^+$ axon fibers. (I) $MAP2^+/NeuN^+$ neurons. (J) $TUJ1^+/TH^+$ dopaminergic neuron at 21 days of differentiation. (K and L) $vGlut2^+/MAP2^+$ glutamatergic neuron at 21 days of differentiation. The image in (L) was high magnification of the white box in (K).

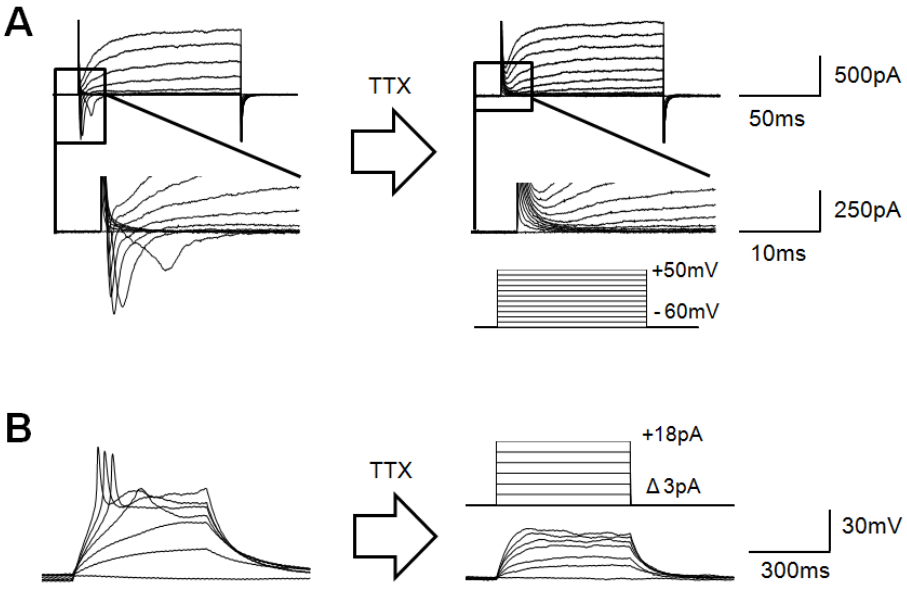

Figure 13. Functionality of the Differentiated Neurons

(A) Na^+ channel-mediated current was examined to prove the functionality of the differentiated neurons. Na^+ currents were produced in neurons. Voltage steps from -60mV to +50mV were applied to the patched cells, and several positive currents were found (*left*, n= 3 cells/total 15 cells). By applying 0.5μM TTX, a Na^+ channel blocker, currents were totally abolished (*right*). Boxes were amplified to show Na^+ currents and their disappearance precisely. (B) Action potentials were also generated in differentiated neurons. Narrow spikes were recorded in the cells which showed Na^+ currents (*left*). Protocol involved sequential steps in stimulation (*right, top*). Detected action potential spikes were also blocked by TTX, just as Na^+ current in (A) (*right, bottom*).

6. Functional and Structural Recovery in a Mouse Model of SCI

To investigate whether transplantation of diPSC-NPCs enhanced functional recovery of the hind limbs of mice with spinal cord injury, both the open field locomotor test (every week) and foot print analysis (final week) were performed. In the open field locomotor test, diPSC-NPC transplantation significantly reversed hind limb dysfunction compared with the control (PBS-injected) group. The transplanted mice frequently showed plantar stepping with weight support (Fig.14). In foot print analysis, diPSC-NPC-transplanted mice had greatly improved walking performance on plantar stepping compared to PBS-injected mice, as judged by the significant increase in the base, stance, and stride lengths (Fig.15). These results indicated that transplantation of the diPSC-NPCs ameliorated the hindlimb dysfunction caused by SCI.

Next, we investigated whether transplantation of diPSC-NPCs reduced spinal cord atrophy in the SCI mouse model by measuring the cross-sectional area of the spinal cord stained with DAPI, a nucleus-staining fluorochrome. The DAPI-positive cross-sectional area gradually declines toward the injury epicenter in spinal cord atrophy. In the diPSC-NPC-transplanted mice, the cross-sectional area at each level was significantly larger than in the PBS-injected mice, suggesting that the transplanted diPSC-NPCs played a beneficial role in structural recovery from SCI (Fig.16).

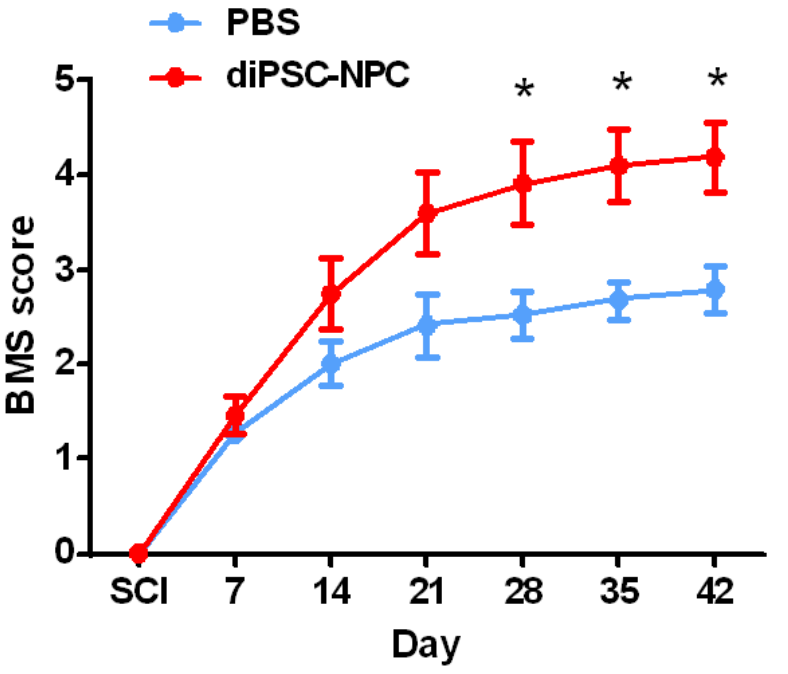

Figure 14. Functional Recovery (BMS score)

BMS scores showed a significant functional recovery of hind limbs in the diPSC-NPC-transplanted group (PBS-control group: n=14, diPSC-NPC group: n=20). *$p<0.05$. Data are presented as the mean ±S.E.M.

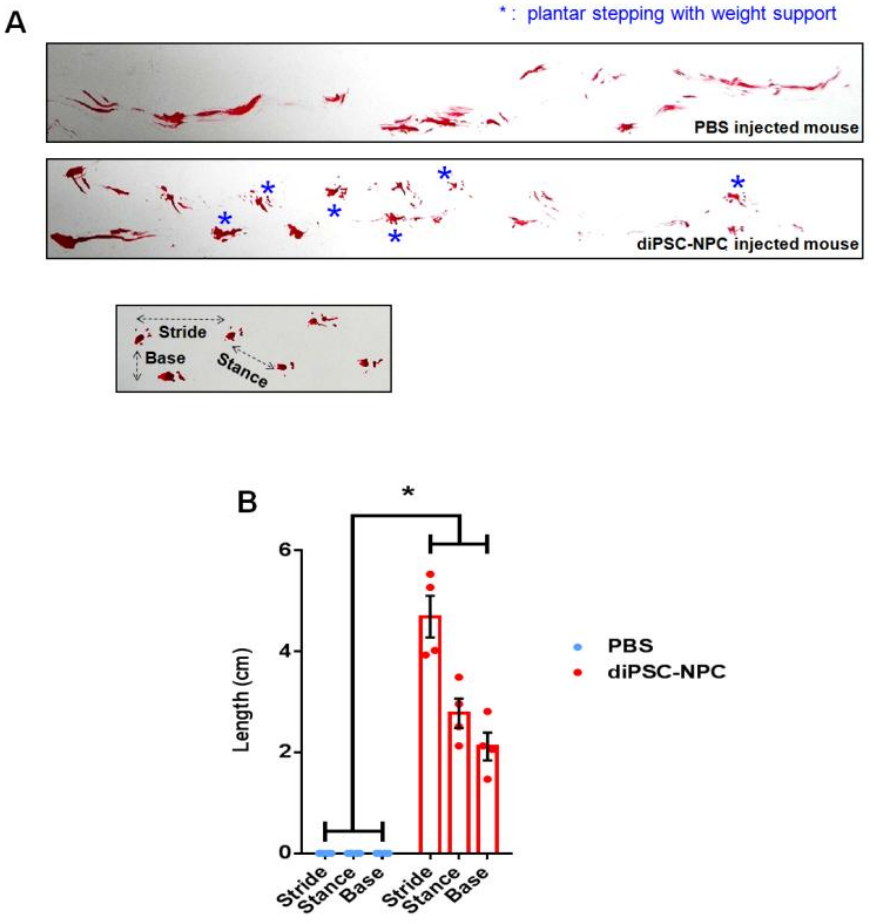

Figure 15. Functional Recovery (Footprint Analysis)

(A) Footprint analysis showed that the diPSC-NPC-transplanted mice displayed better walking performance (plantar stepping, blue asterisk) than the control group. (B) The lengths of base, stride, and stance were also significantly increased in the diPSC-NPC-transplanted group compared with the control group. *$p<0.05$. Data are presented as the mean ±S.E.M.

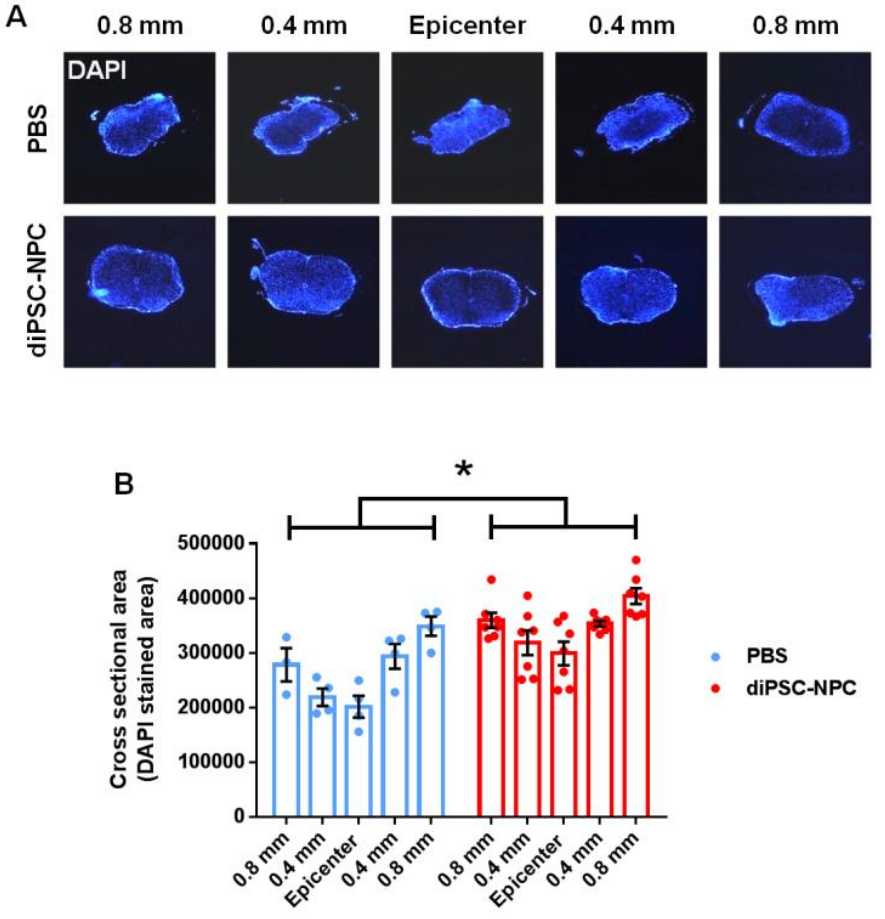

Figure 16. Structural Recovery

(A) Serial cross-sections of spinal cord were stained with DAPI. (B) Measurement of $DAPI^+$ areas of spinal cord cross-sections within 1.6mm (with the injury epicenter in the middle) in the anterior-posterior axis. *$p<0.05$. Data are presented as the mean ±S.E.M.

7. Differentiation of diPSC-derived NPCs *in vivo*

Five weeks post-transplantation, we examined whether the transplanted diPSC-NPCs differentiated into neural cells. The transplanted human diPSC-NPCs could be distinguished from the endogenous mouse cells using human specific nuclei (HNU) antibody. Our results indicated that a significant portion of the transplanted cells were immunoreactive to human-specific nestin antibody (~26.5%), TUJ1 (~30.32%), and MAP2 (~29.5%), suggesting that the injected NPCs either remained NPCs (Fig.17A and B) or differentiated into neurons (Fig.17C-F). Differentiation of the injected diPSC-NPCs into astrocytes (Fig.17G) and oligodendrocyte progenitor cells (Fig.17H) seemed to occur rarely because few HNU and GFAP (astrocyte markers) double-positive cells or HNU and NG2 (oligodendrocyte markers) double-positive cells were observed, respectively (Fig.17G and H). In summary, our results demonstrated that the transplanted diPSC-NPCs preferentially differentiated into neurons *in vivo* and may have eventually resulted in functional recovery in a mouse model of SCI.

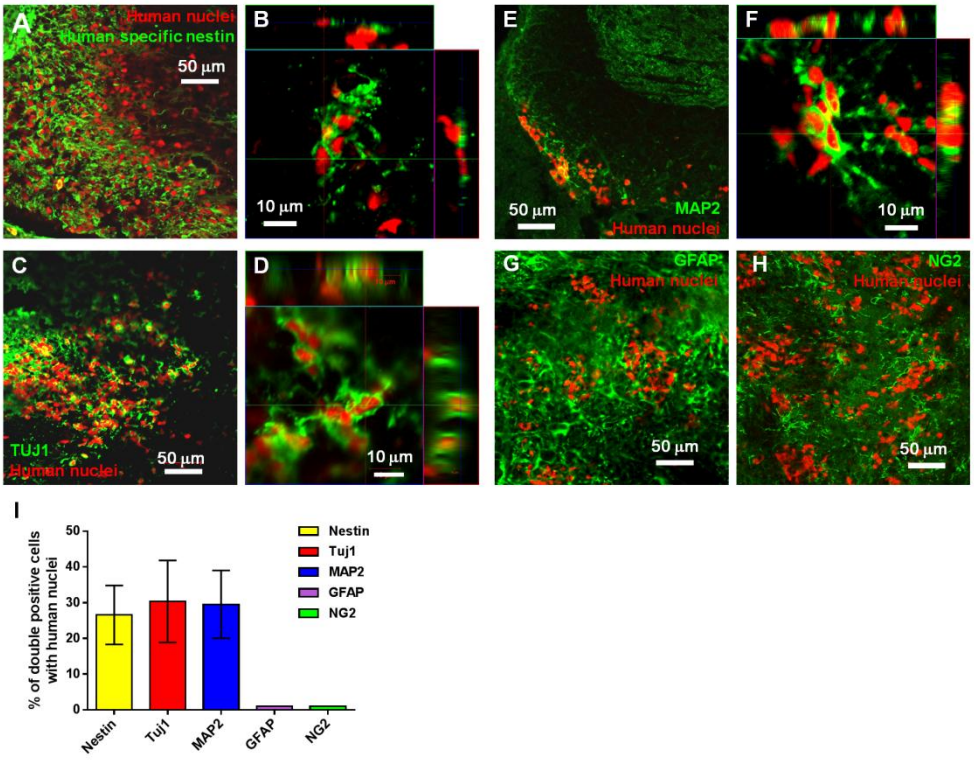

Figure 17. Fate of diPSC-NPCs Transplanted into the Injured Spinal Cord

(A) Immunostaining was performed with antibodies for human nuclei and human-specific nestin. (B) Z-axis scanning of human nuclei and human-specific nestin double-positive cells. (C) Human nuclei and TUJ1-expressing were detected by immunostaining. (D) Z-axis scanning of human nuclei and TUJ1 double-positive cells. (E) Human nuclei and MAP2 double-positive cells were examined. (F) Z-axis scanning of human nuclei and MAP2 double-positive cells. (G) Immunostaining with antibodies specific for human nuclei and GFAP. (H) Immunostaining with antibodies specific for human nuclei and NG2. (I) Percentage of specific cell types derived from transplanted diPSC-NPCs (human nuclei^{+}). Data are presented as the mean ±S.E.M.

Table 4. List of Primer Pairs used in This Study

Gene	Forward primer (5' – 3')	Reverse primer (5' – 3')
Sox1	caatgcggggaggagaagtc	ctctggaccaaactgtggcg
Pax6	ggcaacctacgcaagatggc	tgagggctgtgtctgttcgg
PLZF	ctatgggcgagaggagagtg	tcaatacagcgtcagccttg
DACH1	gtggaaaacacccctcagaa	cttgttccacattgcacacc
PLAGL1	gcctcagtcacctcaaaagc	cttaccctgtggggcaaaga
NR2F	acaggaactgtcccatcgac	gatgtagccggacaggtagc
Endo *Oct4*	gacaggggggaggggaggagctagg	cttccctccaaccagttgccccaaac
Endo *Sox2*	gggaaatgggaggggtgcaaaagagg	ttgcgtgagtgtggatgggattggtg
Endo *Klf4*	acgatcctggccccggaaaaggacc	tgattgtagtgctttctggctgggctcc
Endo *c-Myc*	gcgtcctgggaagggagatccggagc	ttgaggggcatcgtcgcgggaggctg
Trans *Oct4*	ccccagggccccattttggtacc	attttatcgtcgaccactgtgctg
Trans *Sox2*	ggcacccctggcatggctcttggctc	attttatcgtcgaccactgtgctg
Trans *Klf4*	acgatcctggccccggaaaaggacc	attttatcgtcgaccactgtgctg
Trans *c-Myc*	caacaacccaaaatgcaccagccccag	attttatcgtcgaccactgtgctg

Table 5. List of the Antibodies used in This Study

Antibody (Host)	Company	Cat. No	Dilution factor
TUJ1 (Chicken)	Millipore	AB9354	1:1000
TUJ1 (Rabbit)	Abcam	AB18207	1:1000
MAP2 (Mouse)	Abcam	AB11267	1:500
NCAM (Rabbit)	Abcam	AB75813	1:200
NF (Chicken)	Abcam	AB4680	1:1000
NeuN (Rabbit)	Millipore	ABN78	1:1000
vGlut2 (Rabbit)	Abcam	AB101756	1:1000
TH (Mouse)	Millipore	MAB318	1:200
Nestin (Rabbit)	Millipore	ABD69	1:1000
GFAP (Rabbit)	Abcam	AB7260	1:1000
HNU (Mouse)	Millipore	MAB1281C3	1:200
Oct4 (Mouse)	Santa Cruz	SC-5279	1:500
Sox2 (Rabbit)	Cell signaling	#3579	1:500
SSEA4 (Mouse)	Millipore	MAB4304	1:500
Tra1-60 (Mouse)	Millipore	MAB4360	1:500
Tra1-81 (Mouse)	Millipore	MAB4381	1:500
Nestin (Rabbit)	Millipore	MAB5326	1:1000
TUJ1 (Mouse)	Covance	MMS-435P	1:1000
SMA (Mouse)	AbFrontier	YF-PA23164	1:500
PECAM (Mouse)	Millipore	MAB1393	1:500
AFP (Mouse)	Abcam	AB3980	1:500
FoxA2 (Mouse)	AbFrontier	YF-MA10439	1:500
Pax6 (Chicken)	DSHB	Kawakami, A	1:200
Sox1 (Rabbit)	Millipore	AB15766	1:200
NG2 (Rabbit)	Millipore	AB5320	1:200

IV. DISCUSSION

To date, a variety of somatic cell types have been used to generate human iPSCs: fibroblasts [5, 9, 17-21], circulating T cells [9, 10, 22], cord blood stem cells [20, 23], neural stem cells [24], molar mesenchymal stromal cells [25], aortic smooth muscle cells [26], keratinocytes [6], and melanocytes [27]. Intriguingly, certain populations of somatic cells have their own unique characteristics with regards to reprogramming capability, resulting in variable experimental schedules and outcomes in iPSC generation. For example, only Oct4 was required to reprogram neural stem cells into iPSCs [24], and ketatinocytes were approximately100-fold more efficient at iPSC generation than fibroblasts [6].

In most cases, patient-specific iPSCs were generated using fibroblasts obtained from the patient by a punch skin biopsy because of convenience. However, this biopsy involves a painful surgical procedure and requires a significant amount of time to expand the cell population sufficiently for iPSC generation. Therefore, it is of great use to take advantage of "to-be-discarded" tissues obtained from a surgical operation as a source of somatic cells for iPSC-based, patient-specific cell therapy. Our study proposed a paradigm of iPSC generation using waste tissue from emergency surgery on a patient suffering from SCI.

Human intervertebral disc cells are difficult to obtain in normal situations, and there have been no reports describing the use of disc-derived cells for iPSC generation. However, during emergency surgery on SCI patients, this disc tissue is often removed as to-be-discarded "waste" and can be a useful source for iPSC-based autologous cell replacement therapy.

We showed that disc cells derived from the intervertebral disc removed from a SCI patient abundantly expressed disc cell marker genes such as *aggrecan*, *Sox9*, and *Col2A1*. Genome-wide gene expression profile analysis demonstrated a robust expression of chondrocyte genes, further supporting that the cells were derived from the intervertebral disc. The disc cells were efficiently reprogrammed to iPSCs (named

"diPSCs") that successfully met all the criteria of pluripotent stem cells. Therefore, diPSCs originating from the intervertebral disc of a SCI patient will provide a useful therapeutic paradigm for the treatment of SCI in the future.

The diPSCs were readily converted to NPCs by a modified EB-mediated neural differentiation method with dual-smad inhibition [28]. Neural rosette formation and expression of neural markers were comparable between the NPCs derived from H9-hESCs and from diPSCs. In poly-l-ornithine/laminin-coated dishes with neurobasal/B27-based medium, the diPSC-NPCs were efficiently differentiated into neurons. We detected some glutamatergic neurons expressing vGlut2 and also TH^+ dopaminergic neurons. On the contrary, serotonergic neurons and GABAergic neurons were rarely detected (data not shown). In order to examine the functionality of the neurons derived from diPSC-NPCs, we performed whole-cell patch clamp at three weeks after differentiation of NPCs. Our results showed that the differentiated neurons have enough voltage-gated Na^+ channels to mediate the generation of action potentials and Na^+ currents. This result is consistent with previous studies that also recorded Na^+ currents and action potentials to identify NPC differentiation level [29, 30].

When transplanted into the spinal cord of a SCI mouse model, a large number of engrafted NPCs were still alive 5 weeks after transplantation. Intriguingly, a significant portion of the HNU^+ cells were found to be $nestin^+$ NPCs (~26.5%), $TUJ1^+$ neurons (~30.32%), and $MAP2^+$ neurons (~29.5%); only a small number of the engrafted diPSC-NPCs differentiated into astrocytes ($GFAP^+$) and oligodendrocyte progenitor cells ($NG2^+$). These results are similar to those of another group who reported that the engraftment of hiPSC-derived neurospheres produced $nestin^+$ NPCs (~10.7%), $TUJ1^+$ neurons (~49.1%), and APC^+ oligodendrocytes (~3%) [4]. However, this group detected approximately 17% $GFAP^+$ astrocytes, which is significantly higher than what we observed. We speculate that this discrepancy might be caused by differences in the state of engrafted cells (NPCs vs. neurospheres), experimental schedule (analyzed at 35 days vs. 47 days post-transplantation), and the environment surrounding the engrafted cells. In fact, a significant discrepancy has been reported in

differentiation capability between NPCs transplanted into the lesion epicenter and NPCs engrafted onto the edge of injury epicenter [31], and the percentage of neural cell types has been shown to differ depending on length of time to analysis after transplantation [4].

Intriguingly, behavioral amelioration was evident despite the low capability of differentiation into oligodendrocytes in our study and in reports from other groups [4, 32]. Since remyelination of axons by oligodendrocytes is one of the essential processes required for behavioral recovery after SCI, it is tempting to speculate that secreted factor(s) from the engrafted NPCs or their differentiated derivatives may induce endogenous oligodendrocyte-mediated remyelination.

Although tumorigenic potential has been regarded as the most serious issue in ESC and iPSC transplantation research, no tumor formation was observed in this study. This observation is consistent with the absence of $Oct4^+$ cells in the diPSC1-NPC culture at passage 8 (data not shown), suggesting that diPSCs were all differentiated by the neural differentiation protocol used in this study.

Our study demonstrated that surgically removed, to-be-discarded "waste" tissue can be reused to form patient-specific iPSCs. Cells obtained from an emergency surgery, especially those that are difficult to access in normal situations, are a valuable resource for studying cell-specific reprogramming processes, eventually deepening our understanding of the cellular reprogramming process. Furthermore, disc cell-derived iPSCs may be used for autologous cell replacement therapy to treat patients suffering from SCI.

V. CONCLUSION

In this study, iPSCs were generated from human intervertebral disc tissue removed surgically to stabilize the spine after SCI. We confirmed that chondrogenic intervertebral disc cells were completely changed to pluripotent stem cells. The characteristics of the disc cell-derived iPSCs were similar to those of hESCs, but were different from the original disc cells. diPSC-NPCs were efficiently coaxed into mature neurons with the typical action potential of neurons. We confirmed *in vivo* that transplantation of diPSC-NPCs improved the functional recovery of spinal cord injured mice and prevented spinal cord atrophy. A large number of transplanted diPSC-NPCs either remained nestin^{+} NPCs or differentiated into TUJ1^{+} and/or MAP2^{+} neurons. No tumor formation was observed in our study. These findings suggest that to-be-discarded tissues removed from a surgery can be a valuable source for autologous cell replacement therapy.

VI. REFERENCES

1. Takahashi K, Yamanaka S. Induction of pluripotent stem cells from mouse embryonic and adult fibroblast cultures by defined factors. Cell 2006;126:663-76.
2. Rhee Y-H, Ko J-Y, Chang M-Y, Yi S-H, Kim D, Kim C-H, et al. Protein-based human iPS cells efficiently generate functional dopamine neurons and can treat a rat model of Parkinson disease. J Clin Invest 2011;121:2326-35.
3. Hester ME, Murtha MJ, Song S, Rao M, Miranda CJ, Meyer K, et al. Rapid and efficient generation of functional motor neurons from human pluripotent stem cells using gene delivered transcription factor codes. Mol Ther 2011;19:1905-12.
4. Nori S, Okada Y, Yasuda A, Tsuji O, Takahashi Y, Kobayashi Y, et al. Grafted human-induced pluripotent stem-cell–derived neurospheres promote motor functional recovery after spinal cord injury in mice. Proc Natl Acad Sci U S A 2011;108:16825-30.
5. Takahashi K, Tanabe K, Ohnuki M, Narita M, Ichisaka T, Tomoda K, et al. Induction of pluripotent stem cells from adult human fibroblasts by defined factors. Cell 2007;131:861-72.
6. Aasen T, Raya A, Barrero MJ, Garreta E, Consiglio A, Gonzalez F, et al. Efficient and rapid generation of induced pluripotent stem cells from human keratinocytes. Nat biotechnol 2008;26:1276-84.
7. Sun N, Panetta NJ, Gupta DM, Wilson KD, Lee A, Jia F, et al. Feeder-free derivation of induced pluripotent stem cells from adult human adipose stem cells. Proc Natl Acad Sci U S A 2009;106:15720-5.
8. Loh Y-H, Hartung O, Li H, Guo C, Sahalie JM, Manos PD, et al. Reprogramming of T cells from human peripheral blood. Cell Stem Cell 2010;7:15-9.
9. Staerk J, Dawlaty MM, Gao Q, Maetzel D, Hanna J, Sommer CA, et al.

Reprogramming of peripheral blood cells to induced pluripotent stem cells. Cell Stem Cell 2010;7:20-4.

10. Seki T, Yuasa S, Oda M, Egashira T, Yae K, Kusumoto D, et al. Generation of induced pluripotent stem cells from human terminally differentiated circulating T cells. Cell Stem Cell 2010;7:11-4.
11. Mothe AJ, Tator CH. Advances in stem cell therapy for spinal cord injury. J Clin Invest 2012;122:3824-34.
12. Li J, Lepski G. Cell transplantation for spinal cord injury: a systematic review. BioMed Res Int 2013;2013:786475.
13. Kim HT, Lee KI, Kim DW, Hwang DY. An ECM-based culture system for the generation and maintenance of xeno-free human iPS cells. Biomaterials 2013;34:1041-50.
14. Tang X, Richardson WJ, Fitch RD, Brown CR, Isaacs RE, Chen J. A new non-enzymatic method for isolating human intervertebral disc cells preserves the phenotype of nucleus pulposus cells. Cytotechnology 2013:1-8.
15. Sive J, Baird P, Jeziorsk M, Watkins A, Hoyland J, Freemont A. Expression of chondrocyte markers by cells of normal and degenerate intervertebral discs. Mol Pathol 2002;55:91-7.
16. Cho M-S, Hwang D-Y, Kim D-W. Efficient derivation of functional dopaminergic neurons from human embryonic stem cells on a large scale. Nat Protoc 2008;3:1888-94.
17. Yu J, Vodyanik MA, Smuga-Otto K, Antosiewicz-Bourget J, Frane JL, Tian S, et al. Induced pluripotent stem cell lines derived from human somatic cells. Science 2007;318:1917-20.
18. Sugii S, Kida Y, Kawamura T, Suzuki J, Vassena R, Yin Y-Q, et al. Human and mouse adipose-derived cells support feeder-independent induction of pluripotent stem cells. Proc Natl Acad Sci U S A 2010;107:3558-63.
19. Liu H, Ye Z, Kim Y, Sharkis S, Jang YY. Generation of endoderm- derived human induced pluripotent stem cells from primary hepatocytes. Hepatology

2010;51:1810-9.

20. Ye Z, Zhan H, Mali P, Dowey S, Williams DM, Jang Y-Y, et al. Human-induced pluripotent stem cells from blood cells of healthy donors and patients with acquired blood disorders. Blood 2009;114:5473-80.
21. Loh Y-H, Agarwal S, Park I-H, Urbach A, Huo H, Heffner GC, et al. Generation of induced pluripotent stem cells from human blood. Blood 2009;113:5476-9.
22. Brown ME, Rondon E, Rajesh D, Mack A, Lewis R, Feng X, et al. Derivation of induced pluripotent stem cells from human peripheral blood T lymphocytes. PLOS ONE 2010;5:e11373.
23. Eminli S, Foudi A, Stadtfeld M, Maherali N, Ahfeldt T, Mostoslavsky G, et al. Differentiation stage determines potential of hematopoietic cells for reprogramming into induced pluripotent stem cells. Nat Genet 2009;41:968-76.
24. Kim JB, Greber B, Araúzo-Bravo MJ, Meyer J, Park KI, Zaehres H, et al. Direct reprogramming of human neural stem cells by OCT4. Nature 2009;461:649-53.
25. Oda Y, Yoshimura Y, Ohnishi H, Tadokoro M, Katsube Y, Sasao M, et al. Induction of pluripotent stem cells from human third molar mesenchymal stromal cells. J Biol Chem 2010;285:29270-8.
26. Lee T-H, Song S-H, Kim KL, Yi J-Y, Shin G-H, Kim JY, et al. Functional recapitulation of smooth muscle cells via induced pluripotent stem cells from human aortic smooth muscle cells. Circ Res 2010;106:120-8.
27. Utikal J, Maherali N, Kulalert W, Hochedlinger K. Sox2 is dispensable for the reprogramming of melanocytes and melanoma cells into induced pluripotent stem cells. J Cell Sci 2009;122:3502-10.
28. Chambers SM, Fasano CA, Papapetrou EP, Tomishima M, Sadelain M, Studer L. Highly efficient neural conversion of human ES and iPS cells by dual inhibition of SMAD signaling. Nat Biotechnol 2009;27:275-80.

29. Chanda S, Marro S, Wernig M, Südhof TC. Neurons generated by direct conversion of fibroblasts reproduce synaptic phenotype caused by autism-associated neuroligin-3 mutation. Proc Natl Acad Sci U S A 2013;110:16622-7.

30. Vierbuchen T, Ostermeier A, Pang ZP, Kokubu Y, Südhof TC, Wernig M. Direct conversion of fibroblasts to functional neurons by defined factors. Nature 2010;463:1035-41.

31. Iwai H, Nori S, Nishimura S, Yasuda A, Takano M, Tsuji O, et al. Transplantation of neural stem/progenitor cells at different locations in mice with spinal cord injury. Cell Transplant 2013.

32. Fujimoto Y, Abematsu M, Falk A, Tsujimura K, Sanosaka T, Juliandi B, et al. Treatment of a Mouse Model of Spinal Cord Injury by Transplantation of Human Induced Pluripotent Stem Cell- Derived Long Term Self Renewing Neuroepithelial- Like Stem Cells. Stem Cells 2012;30:1163-73.

ABSTRACT (IN KOREAN)

척수손상 후 신경학적 기능 장애를 개선하기 위한 인간 추간판 세포 유래 유도만능줄기세포

<지도교수 윤도흠>

연세대학교 대학원 의과학과

오 진 수

유도만능줄기세포는 환자 맞춤형 세포 치료에 사용 될 수 있는 가장 전망 있는 줄기세포이며 현재까지 섬유아세포와 혈액 세포와 같은 다양한 체세포를 이용하여 유도만능줄기세포를 제작한 사례가 있다. 하지만, 대부분의 척수손상이 교통사고, 낙상 등에 의해 골절된 척추가 척수신경에 손상을 주어 발생한다는 점을 고려하여, 본 연구에서는 척수 손상 후 척추 융합 수술을 받는 과정에서 제거된 디스크 조직을 사용하여 유도만능줄기세포를 제작하였다. 이렇게 제작된 유도만능줄기세포가 척수 손상 치료를 위해 사용될 재료로서 적합한지 여부를 평가하기 위해 유도만능줄기세포의 만능성과 신경전구세포로의 분화능 등을 조사하였다.

다양한 분석을 통해 우리는 인간 디스크조직 유래 유도만능줄기세포가 인간 배아줄기세포와 매우 유사한 특징을 갖고 있다는 것을 확인하였고, 제작한 유도만능줄기세포는 성숙한 신경세포로 분화가 가능한 신경전구세포로 분화될 수 있음을 확인하였다.

환자의 디스크 조직으로 제작한 유도만능줄기세포 유래 신경전구세포의 치료 효과를 확인하기 위해, 마우스 척수손상 모델을 제작하고 9일 후에 손상 받은 척수에 신경전구세포를 직접 이식하였다. 신경전구세포의 이식은 척수 손상 마우스의 운동 기능 회복을 크게 향상 시켰고, 2차 손상으로 야기되는 척수 위축 현상을 보호하였다. 이식 5주 후 조직학적 분석을 통해 우리는 이식한 신경전구세포의 대부분이 nestin 항체 양성의 신경전구세포 상태로 남아있거나, TUJ1과 MAP2 항체 양성의 신경세포로 각각 분화된 것을 관찰 할 수 있었다.

본 연구에서 우리는 수술과정 중에 제거된 환자의 디스크 조직이 환자 맞춤형 유도만능줄기세포 제작을 위해 재사용 될 수 있다는 것을 증명하였고, 척수 손상 모델에서 유도만능줄기세포 유래 신경전구세포의 치료 효과를 보여주었다.

핵심되는 말: 디스크 조직, 유도만능줄기세포, 신경전구세포, 세포 이식, 척수 손상